ACCSCIENCE PUBLISHING

International Journal of Bioprinting

RESEARCH ARTICLE

3D-bioprinted cell-laden hydrogel with anti-inflammatory and anti-bacterial activities for tracheal cartilage regeneration and restoration

Pengli Wang[1†], Tao Wang[1†], Yong Xu[1*], Nan Song[1*], and Xue Zhang[2*]

[1]Department of Thoracic Surgery, Shanghai Pulmonary Hospital, Tongji University School of Medicine, Shanghai 200430, China

[2]Dermatology Center, Xinhua Hospital, Shanghai Jiaotong University School of Medicine, Shanghai 200092, China

(This article belongs to the *Special Issue: Advances in 3D bioprinting for regenerative medicine and drug screening*)

Abstract

Despite the notable advances in tissue-engineered tracheal cartilage (TETC), there remain several challenges that need to be addressed, such as uneven cell distribution for cartilage formation, customized C-shaped tracheal morphology, local inflammatory reactions, and infections. To overcome these challenges, this study proposed the addition of icariin (ICA) and chitosan (CS) into a gelatin methacryloyl (GelMA) hydrogel to develop a new ICA/CS/GelMA hydrogel with anti-inflammatory and anti-bacterial properties, and three-dimensional (3D)-bioprinting feasibility. The aim of this study was to construct a TETC, a customized C-shaped cartilage structure, with uniform chondrocyte distribution as well as anti-inflammatory and anti-bacterial functions. Our results confirmed that ICA/CS/GelMA hydrogel provides desirable rheological properties, suitable printability, favorable biocompatibility, and simulated microenvironments for chondrogenesis. Moreover, the addition of ICA stimulated chondrocyte proliferation, extracellular matrix synthesis, and anti-inflammatory ability, while the encapsulation of CS enhanced the hydrogels' anti-bacterial ability. All these led to the formation of an enhanced TETC after submuscular implantation and an elevated survival rate of experimental rabbits after orthotopic tracheal transplantation. This study provides a reliable cell-laden hydrogel with anti-inflammatory and anti-bacterial activities, suitable printability, and significant advancements in *in vivo* cartilage regeneration and *in situ* tracheal cartilage restoration.

Keywords: 3D bioprinting; Anti-inflammation; Anti-bacteria; Cartilage regeneration; Tracheal restoration

1. Introduction

Recently, various novel strategies, including intact cartilaginous tubes[1,2], assembled tubes with interrupted O-shaped[3-5], and C-shaped cartilaginous rings[6], have been explored extensively to construct tissue-engineered tracheal cartilage (TETC) to repair long-segmental tracheal defects. However, tracheal cartilage regeneration and restoration still face numerous challenges that need to be addressed, such as uneven cell distribution

†These authors contributed equally to this work.

***Corresponding authors:**
Yong Xu
(xuyong@tongji.edu.cn)

Nan Song
(songnan@tongji.edu.cn)

Xue Zhang
(xuezhang@shsmu.edu.cn)

Citation: Wang P, Wang T, Xu Y, *et al*., 2023, 3D-bioprinted cell-laden hydrogel with anti-inflammatory and anti-bacterial activities for tracheal cartilage regeneration and restoration. *Int J Bioprint*. https://doi.org/10.36922/ijb.0146

Received: April 27, 2023
Accepted: May 28, 2023
Published Online: July 13, 2023

for homogeneous cartilage formation[7], difficulty in customizing tracheal morphology, precise regeneration of C-shaped tracheal cartilage[8], local inflammatory reactions caused by surgical trauma, introduced scaffolds that inevitably compromise the structure and functionality of TETC[9], and infection caused by respiratory microbiota that may further lead to TETC deterioration[10,11]. Therefore, there is still a need for new strategies to construct TETC with uniform chondrocyte distribution, customized cartilage shape, as well as anti-inflammatory and anti-bacterial functions.

The routine method for constructing a TETC involves seeding chondrocytes onto a porous scaffold[12]. However, uneven cell distribution and chondrocyte waste caused by the turbulent flow of the cell seeding suspension limit its further application[13-15]. Three-dimensional (3D) bioprinting is an emerging technology that provides precise control over the fabricated constructs, including cell distribution and structure[16]. Park *et al.* presented an advanced extrusion-based 3D-bioprinting strategy involving a two-step printing process: (i) printing a porous bellows framework and (ii) printing the cartilage rings[17]. In our previous study, we successfully developed a 3D-bioprinted tracheal tissue incorporating O-shaped cartilage, providing further evidence of the capability of 3D-bioprinting technology to achieve uniform cell distribution and precise shape control[18]. However, recent advancements from our research group have demonstrated that a C-shaped cartilage configuration can more accurately mimic the structure and function of native tracheal cartilage, resulting in enhanced tracheal cartilage formation and restoration of tracheal defects. Notably, the mentioned study employed a method involving the direct injection of cell-loaded hydrogel into customized C-shaped molds to create the C-shaped cartilage[6]. Nevertheless, this approach presents limitations when constructing long-segmental tissue-engineered tracheal constructs with patient-specific shapes. Moreover, the mold-based method is intricate, time-consuming, and associated with a low success rate, thereby greatly restricting its practicality in applications. Therefore, it remains crucial to investigate the feasibility of utilizing 3D-bioprinting technology to construct tissue-engineered tracheal constructs with precise C-shaped cartilage structures. Additionally, compared to 3D bioprinting a trachea-mimetic cellular construct, the process of 3D bioprinting a single C-shaped cell-laden hydrogel ring requires less printing time, which can contribute to improved chondrocyte viability and survival[17].

However, despite advancements in developing TETC using various techniques, including 3D bioprinting and scaffold-based approaches, several challenges remain. One critical issue is the susceptibility of TETC to inflammation after *in vivo* implantation, caused by local inflammatory reactions resulting from surgical trauma and introduced materials, and further exacerbated by respiratory microbiota[19-21]. The tracheal ciliated epithelial tissue layer plays a crucial role in protecting cartilaginous tissue against inflammatory and bacterial invasion[22-24]. Our previous study demonstrated that re-epithelialization promotes TETC regeneration, but self-migration is not a reliable and effective method, especially for long-segmental tracheal defects[3]. Existing studies have attempted to address this issue by preparing a sinusoidal-patterned tubular mesh or developing a porous O-shaped scaffold ring with anti-inflammatory effects[9,17]. However, these studies neglected the importance of anti-bacterial function. Therefore, the current study aimed to develop a hydrogel that could be 3D-bioprinted with cells to generate a precise C-shaped tracheal ring and exert both anti-inflammatory and anti-bacterial functions to enhance TETC formation and tracheal restoration after orthotopic tracheal transplantation.

Icariin (ICA) is a prenylated flavonol glycoside extracted from *Epimedium* that has been shown to have favorable anti-inflammatory and chondroprotective effects by modulating autophagy and apoptosis[25,26]. In addition, a study has suggested that ICA could be used as an alternative to growth factors for TETC regeneration due to its chondrogenic effects[27]. Chitosan (CS) is a natural-derived polysaccharide approved by the U.S. Food and Drug Administration (FDA) for pharmaceutical applications. It has excellent anti-bacterial ability attributed to the binding of its positively charged NH^{3+} groups to negatively charged bacterial surfaces[28]. The anti-bacterial effect of CS is essential in preventing infection due to the bacterial environment of the tracheal lumen. However, poor reproducibility and mechanical properties are insurmountable restrictions of CS-based hydrogels used as bioinks[16]. Gelatin methacryloyl (GelMA) hydrogel has gained increasing attention due to its ability to crosslink and form hydrogels with tunable mechanical properties and excellent biocompatibility, mimicking the microenvironment of the native extracellular matrix (ECM)[29]. In addition to acting as a carrier of cells, GelMA can also serve as a controlled drug delivery system for the administration of various active substances, such as drug molecules[16].

In this study, we propose to enhance the anti-inflammatory and anti-bacterial properties of GelMA by incorporating both ICA and CS. Our objective is to develop an ICA/CS/GelMA hydrogel that can be utilized in the fabrication of a TETC. We hypothesize that this hydrogel can be pre-loaded with chondrocytes and subjected to a 3D-bioprinting process to create a TETC with a precise C-shaped ring. Doing so, we can address several challenges

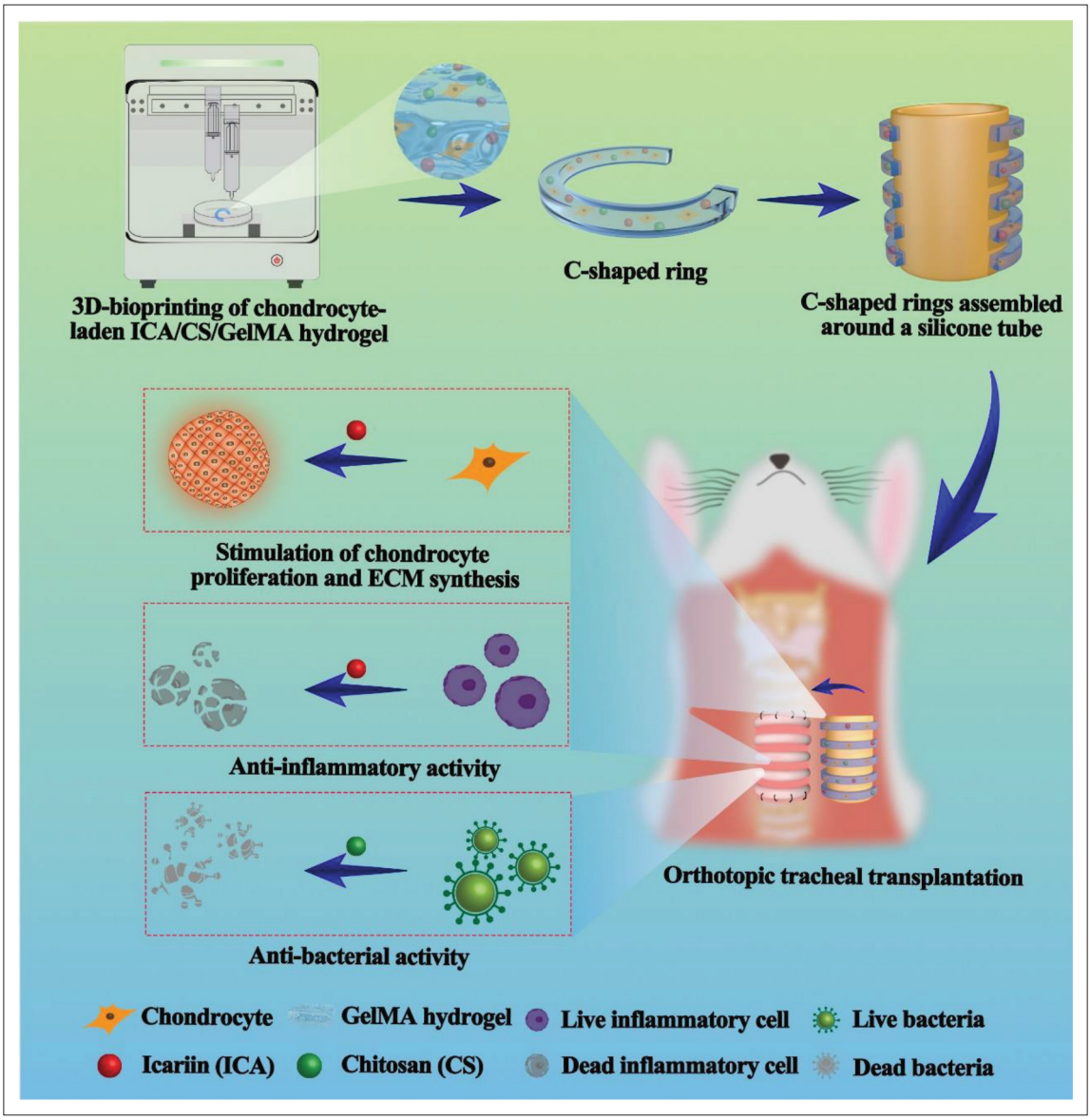

Figure 1. A schematic design of the study. Firstly, GelMA hydrogel was mixed with ICA and CS to create an ICA/CS/GelMA hydrogel with anti-inflammatory and anti-bacterial activities. Chondrocytes were evenly pre-loaded into the hydrogel, and the mixture was then fabricated into a customized C-shaped ring using a 3D-bioprinting technique. To investigate the anti-inflammatory effect of the ICA/CS/GelMA hydrogel, several synthesized C-shaped rings were stacked onto a silicone tube and implanted into the platysma of an autologous rabbit to regenerate a TETC over a period of 3 weeks. To evaluate the anti-bacterial function of the ICA/CS/GelMA hydrogel, the TETC was used for orthotopic tracheal defect transplantation in an autologous rabbit model.

in cartilage tissue engineering, including the need for uniform chondrocyte distribution and customized cartilage shape, as well as the provision of anti-inflammatory and anti-bacterial functions. Figure 1 illustrates the overall schematic design of our proposed approach.

2. Materials and methods

2.1. Materials and animals

For this study, we procured several chemicals from Sigma-Aldrich, including gelatin, ICA, CS, lithium phenyl-2,4,6-trimethylbenzoyl-phosphinate (LAP), trypsin, type II collagenase, Triton X-100, methacrylic anhydride, phosphate-buffered saline (PBS), DMEM, and fetal bovine serum (FBS), which were all analytical grade. Additionally, we obtained other reagent-grade chemicals from commercial sources. New Zealand white rabbits, 1 month old, were procured from Shanghai Jiagan Experimental Animal Raising Farm. All animal experimentation procedures were approved by the Ethics Committee of Shanghai Pulmonary Hospital.

Table 1 Primers used in the qPCR

Gene	Forward (5'–3')	Reverse (5'–3')
TNF-α	AGAACAGCAACTCCAGAACACCCT	TGCCAGTTCCACATCTCGGATCAT
IL-6	AGACAGCCACTCACCTCTTCAG	TTCTGCCAGTGCCTCTTTGCTG
GAPDH	CGCTAACATCAAATGGGGTG	TTGCTGACAATCTTGAGGGAG

2.2. Preparation of GelMA, ICA/GelMA, CS/GelMA, and ICA/CS/GelMA hydrogel precursors

To prepare GelMA, we followed the previously described protocol[18]. In brief, we dissolved 10 g of gelatin in 500 mL of PBS (pH = 7.4) and stirred vigorously at 50°C until complete dissolution. Next, we added 10 mL of methacrylate anhydride slowly into the solution and allowed it to react with gelatin for 2 h. After the reaction, we collected the solution and removed insoluble substances by centrifugation at 5000 rpm. The crude product was dialyzed against deionized water at 40°C for 3 days, followed by freezing and lyophilizing. For pristine GelMA hydrogel precursors, we dissolved 10% w/v GelMA and 0.3% w/v LAP (a photoinitiator) in PBS. Then, we separately dissolved 10 μM ICA, 2% w/v CS, and a combination of 10 μM ICA and 2% w/v CS in the pristine GelMA hydrogel precursors to obtain ICA/GelMA, CS/GelMA, and ICA/CS/GelMA hydrogel precursors, respectively.

2.3. Characterizations of hydrogels

2.3.1. Rheological analyses

We conducted dynamic rheological experiments at room temperature using the HAAKE MARS III photorheometer equipped with parallel-plate (P20 TiL, 20 mm diameter) geometry and OmniCure Series 2000 (365 nm, 20 mW/cm^2). During the experiments, we gradually increased the shear rate from 0 to 100 s^{-1} to measure the viscosity of the samples. We also determined the storage modulus (G') and the loss modulus (G") of the hydrogels under UV irradiation (365 nm and 30 mW/cm^2) for 400 s.

2.3.2. Mechanical test

To evaluate the mechanical properties of cylindrical hydrogels, we employed a dynamic mechanical analyzer (Instron-5542; Canton, USA). The samples from all groups were subjected to compression at a rate of 1 mm/min until the depth of compression reached 30% of the initial height. We computed the elastic modulus using the initial 0–20% of the strain–stress curve.

2.4. The evaluation of anti-inflammatory effect

To evaluate the anti-inflammatory effect of the hydrogels, we obtained RAW264.7 murine macrophages from the Type Culture Collection of the Chinese Academy of Sciences and incubated them at 37°C with a 5% CO_2 atmosphere. The RAW264.7 cells were pre-stimulated with lipopolysaccharide (LPS, 100 ng/mL) for 24 h, followed by co-culture with GelMA, ICA/GelMA, CS/GelMA, and ICA/CS/GelMA hydrogels for another 24 h. We analyzed the expression levels of the inflammatory cytokines tumor necrosis factor α (TNF-α) and interleukin 6 (IL-6) in the samples by immunofluorescence staining. The samples were treated overnight with primary antibodies against TNF-α (ab303458, Abcam) and IL-6 (ab183218, Abcam) at 4°C. After rinsing, we treated the samples with goat anti-rabbit secondary antibody (1:1000, ab150077, Abcam) in the dark. Finally, we mounted coverslips with 4′,6-diamidino-2-phenylindole (DAPI, Sigma) mounting solution, visualized them using a fluorescent imaging system, and analyzed them with a fluorescence microscope (Olympus).

To analyze the protein levels of TNF-α and IL-6, we conducted western blotting. We extracted total proteins from RAW264.7 cells using a previously described method[30] and prepared the protein samples. Then, we measured the protein concentrations, added a loading buffer, mixed the protein samples, and boiled them. Next, we isolated the proteins and transferred them onto a membrane, followed by blocking. After that, we immersed the protein strips in primary antibodies (1:1000, Beyotime, Shanghai, China) overnight at 4°C. After washing for 1 h, we incubated the strips with the corresponding secondary antibodies (1:2000; Beyotime, Shanghai, China) and rinsed them thrice (15 min each) with Tris-buffered saline with tween (TBST). Finally, we developed the strips to analyze the protein levels of TNF-α and IL-6, in which β-actin was used as control.

To analyze the gene expression levels of TNF-α and IL-6, we carried out qPCR experiments. We extracted total RNA using TRIzol™ reagent (Invitrogen) and performed cDNA synthesis using Moloney murine leukemia virus reverse transcriptase (Invitrogen). Quantification was carried out using qPCR with the primers listed in Table 1 and a Fast Synergy Brands Green Master Kit and Light Cycler 480 System (Roche) according to the manufacturer's instructions. We used the comparative threshold cycle method to analyze the results and normalized the expression of TNF-α and IL-6 to the endogenous reference gene GAPDH.

2.5. *In vitro* anti-bacterial activity

To test the *in vitro* anti-bacterial activity against gram-positive (*Staphylococcus aureus*) and gram-negative

(*Escherichia coli*) bacteria, we carried out the following procedures. We mixed 80 mg of different hydrogel samples (GelMA, ICA/GelMA, CS/GelMA, and ICA/CS/GelMA) with 200 μL of bacterial solution (1×10^6 cfu/mL) in sterile Eppendorf tubes. Eppendorf tubes containing 200 μL of bacterial solution (blank) only were used as a control. After incubation, we diluted the samples 100-fold and then plated them to observe colony growth. We measured the bacterial-occupied area using the following formula:

$$\frac{\alpha}{\beta} \times 100\%$$

where α is the area of colonies with the treatment of the hydrogel and β is the total area of agar plates.

2.6. Chondrocytes preparation

To obtain chondrocytes for our experiments, we collected auricular cartilage samples from rabbits through surgery. We then digested the samples using 0.15% type II collagenase and cultured the resultant chondrocytes in DMEM containing 10% FBS and 1% penicillin–streptomycin at 37°C in a 5% CO_2 incubator. We used chondrocytes at the second passage (P2) for further experiments.

2.7. Bioprinting of C-shaped rings using cell-laden hydrogels

For 3D bioprinting, we homogeneously mixed chondrocytes in the different hydrogels at a concentration of 1×10^8 cells/mL. The chondrocyte-loaded hydrogels were then loaded into 5 mL syringes equipped with 0.21 mm diameter needles and mounted into the syringe pump extruder on a 3D BioArchitect workstation (Regenovo). The temperatures of the syringes and platform were maintained at 16 ± 1°C. To fabricate a single layer of ring-shaped constructs (9.0 mm external diameter, 6.0 mm internal diameter, and 1.5 mm height for C rings), we printed four layers of each bioink and photocrosslinked them upon light irradiation (365 nm, 20 mW/cm^2) within 30 s. The printing parameters were set as follows: line gap, 400 μm; layer thickness, 400 μm; photocrosslinking time, 30 s per ring; pneumatic pressure, 0.2 MPa; extrusion speed, 1.5 mm^3/s. After printing, we incubated the bioprinted constructs in DMEM supplemented with 10% FBS and 1% penicillin/streptomycin at 37°C and 5% CO_2. We conducted each step under sterile conditions to ensure the integrity of the bioprinted constructs.

2.8. Cell viability, proliferation, and chondrogenesis evaluations

After printing, the cell-laden hydrogels were incubated at 37°C in a 5% CO_2 incubator for 9 days. The culture medium (DMEM supplemented with 10% FBS) was changed every other day. On days 1, 4, and 9, we evaluated the cell viability using the Live/Dead Cell Viability Assay (Invitrogen) following the manufacturer's instructions and examined them using a fluorescence microscope (Olympus). We also assessed cell proliferation via the DNA quantification and Cell Counting Kit-8 (CCK-8) assay to further evaluate the viability of chondrocytes in hydrogels. DNA was quantified using the PicoGreen dsDNA assay kit (Invitrogen, USA) according to the manufacturer's instructions. The CCK-8 assay was performed according to the manufacturer's instructions, and the absorbance was measured at 450 nm using a spectrophotometer.

To evaluate the chondrogenic capacity of the various hydrogels, we cultured the printed cell-laden hydrogels in the culture medium (DMEM supplemented with 10% FBS) for 3 weeks. Then, we analyzed the expression level of collagen type II (COL II) in the samples by immunofluorescence staining, as described in section 2.4. We also quantified the COL II contents using an enzyme-linked immunosorbent assay (ELISA).

2.9. *In vivo* TETC regeneration

To facilitate the *in vivo* regeneration of TETCs, a total of 24 rabbits were randomly assigned to four groups: GelMA, ICA/GelMA, CS/GelMA, and ICA/CS/GelMA, with six rabbits per group. The 3D-printed C-shaped rings in all the cell-laden hydrogel groups were interrupt-stacked onto a silicone tube and implanted into the platysma of anesthetized autologous rabbits. The C-shaped rings underwent 3- or 6-week implantation to generate TETC tissues. The retrieved TETC samples were photographed with an SLR camera for gross observation and sectioned for histological evaluation, including hematoxylin and eosin (H&E), safranin-O, and immunohistochemical staining for COL II. Glycosaminoglycan (GAG) and COL II contents were quantified using the dimethylmethylene blue assay (DMMB, Sigma-Aldrich) and ELISA, respectively.

Moreover, the expression levels of TNF-α and IL-6, as well as an apoptosis-related marker (TUNEL) in the samples, were analyzed by immunofluorescence staining, as described in section 2.4. A TUNEL apoptosis detection kit (C1086; Beyotime, Shanghai, China) was used to detect apoptotic cells by immunofluorescence staining. The acquired images were analyzed using ImageJ software to calculate the relative intensity. Specifically, we used the formula $\alpha/\beta \times 100\%$, where α represents the occupied area of the positive expressed marker, and β represents the area of the total image.

2.10. Orthotopically transplantation of TETC in autologous rabbits

The TETCs generated in the ICA/GelMA and ICA/CS/GelMA groups (as described in section 2.9) were orthotopically transplanted into the 0.6-cm-long native

tracheal defect of rabbits. The TETCs were intermittently sutured using 5-0 monofilament COVIDIEN sutures, and the survival rate of experimental rabbits in both groups was recorded after 8 weeks. At the end of the 3-week transplantation, the experimental rabbits in both groups were sacrificed for gross and histological examinations. Immunofluorescence fluorescence *in situ* hybridization (FISH) staining was performed to evaluate bacterial distribution, and the obtained images were used to quantify the bacterial intensity per field. Immunofluorescence staining of COL II was used to evaluate cartilage-related characteristics. COL II contents were quantified using ELISA, and Young's modulus was analyzed using a dynamic mechanical analyzer, as described in section 2.3.2.

2.11. Statistical analysis

Statistical analysis was performed using GraphPad Prism 8 software, with a minimum of three samples per group. Differences between treatments were assessed using one-way ANOVA or unpaired Student's t-test, as appropriate. Results are expressed as mean ± standard deviation (SD), and statistical significance was defined as $P < 0.05$.

3. Results

3.1. Synthesis and characterizations of GelMA, ICA/GelMA, CS/GelMA, and ICA/CS/GelMA hydrogels

To create tissue-specific bioinks, GelMA was used as a substrate, and a photocrosslinking approach was employed to ensure stability for 3D bioprinting[18]. After exposure to UV light (365 nm, 20 mW/cm^2) for 30 s, GelMA, ICA/GelMA, CS/GelMA, and ICA/CS/GelMA hydrogel precursors were rapidly crosslinked (Figure 2a). Additionally, the encapsulation of chondrocytes did not interfere with gelation (Figure 2b). GelMA, ICA/GelMA, CS/GelMA, and ICA/CS/GelMA hydrogels exhibited shear-thinning behavior (Figure 2c), which is critical for an injectable hydrogel to flow continuously. Dynamic modulus (G' and G") of various hydrogels under UV light at different times (Figure 2d) showed that gelation was achieved after photo-triggered crosslinking, and the gelation of the hydrogel could be controlled by adjusting the irradiation time. Mechanical analysis (Figure 2e–f) revealed that all GelMA, ICA/GelMA, CS/GelMA, and ICA/CS/GelMA groups exhibited no significant differences, indicating that the addition of ICA and CS did not affect the mechanical properties of GelMA hydrogel. We designed a customized 3D model for a C-shaped ring (Figure 2g), and our results showed that chondrocyte-laden hydrogels were successfully printed into the C-shaped rings in all GelMA, ICA/GelMA, CS/GelMA, and ICA/CS/GelMA groups (**Videoclip S1** in Supplementary File and Figure 2h). Moreover, the printed C-shaped rings could maintain their original shape after being immersed in PBS solution (**Videoclip S2** in Supplementary File). These findings demonstrated that the synthesized hydrogel is suitable for bioprinting cell-laden constructs.

3.2. *In vitro* anti-inflammatory and anti-bacterial activities of GelMA, ICA/GelMA, CS/GelMA, and ICA/CS/GelMA hydrogels

To evaluate the anti-inflammatory effect of the hydrogels *in vitro*, RAW264.7 macrophages stimulated with LPS were incubated with GelMA, ICA/GelMA, CS/GelMA, and ICA/CS/GelMA hydrogels for 24 h. Compared to the GelMA and CS/GelMA groups, the ICA/GelMA and ICA/CS/GelMA groups exhibited significantly reduced expression of TNF-α and IL-6, the inflammatory cytokines, as confirmed by immunofluorescence staining (Figure 3a–b). Western blot results also showed a significant decrease in relative protein expression of TNF-α and IL-6 in the ICA/GelMA and ICA/CS/GelMA groups compared to the GelMA and CS/GelMA groups (Figure 3c). Additionally, qPCR examination confirmed that the relative gene expression of TNF-α and IL-6 was significantly suppressed in the ICA/GelMA and ICA/CS/GelMA groups compared to the GelMA and CS/GelMA groups (Figure 3d). These results indicate that the addition of ICA enhances the anti-inflammatory effect of GelMA-based hydrogels.

To determine the anti-bacterial activity of the hydrogels *in vitro*, both gram-positive (*S. aureus*) and gram-negative (*E. coli*) bacteria were cultured in Petri dishes and treated with different hydrogels. The GelMA and ICA/GelMA groups exhibited good bacterial viability for both *S. aureus* and *E. coli* compared with the control group, while the CS/GelMA and ICA/CS/GelMA groups demonstrated a significant reduction in bacterial viability for both *S. aureus* and *E. coli* (Figure 4a–b). The quantitative analysis showed that the bacterial survival rate for *S. aureus* and *E. coli* in control, GelMA, and ICA/GelMA groups was higher than that in the CS/GelMA and ICA/CS/GelMA groups, indicating that the addition of CS significantly enhances the anti-bacterial activity.

In conclusion, these results suggest that ICA endows ICA/GelMA and ICA/CS/GelMA hydrogels with significant anti-inflammatory ability, while CS endows CS/GelMA and ICA/CS/GelMA hydrogels with credible anti-bacterial ability.

3.3. Cytocompatibility of GelMA, ICA/GelMA, CS/GelMA, and ICA/CS/GelMA hydrogels

To evaluate the viability, spreading, and proliferation of chondrocytes in the hydrogels, the chondrocyte-laden hydrogels in GelMA, ICA/GelMA, CS/GelMA, and ICA/CS/GelMA groups were cultured *in vitro*. Live/dead staining (Figure 5a) showed that chondrocytes in all groups exhibited high viability with minimal cell death. Notably,

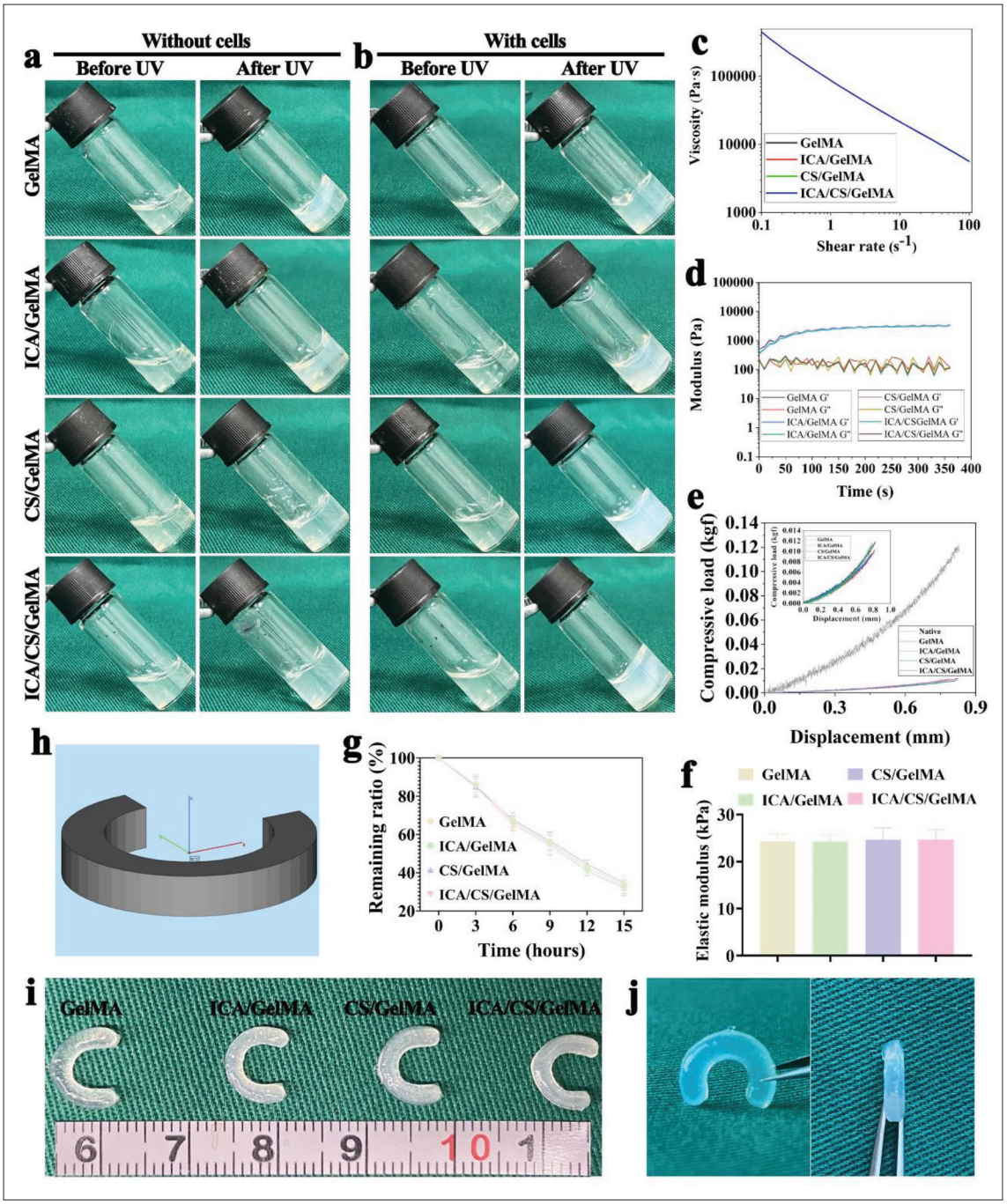

Figure 2. **The characterizations of the ICA/CS/GelMA hydrogel and 3D bioprinting of C-shaped rings.** Photographs of sol-to-gel transition upon UV light irradiation (365 nm, 20 mW/cm^2) were taken (a) without and (b) with cells (1 × 10^8 cells/mL) in GelMA, ICA/GelMA, CS/GelMA, and ICA/CS/GelMA hydrogels. (c) The viscosity of various hydrogels at room temperature was also measured. (d) Dynamic moduli (G' and G") of various hydrogels were measured with UV light at varying times. (e) Stress–strain curves and (f) elastic modulus of various hydrogels were obtained. (g) *In vitro* biodegradability of various hydrogels. (h) 3D modeling of C-shaped ring. (i) Photographs of printed C-shaped rings using various hydrogels pre-loaded with chondrocytes were taken. (j) The photographs of C-shaped rings taken from different positions in ICA/CS/GelMA group.

the ICA/GelMA and ICA/CS/GelMA groups exhibited more live chondrocytes, as evidenced by the increased green staining, than the GelMA and CS/GelMA groups on days 1, 4, and 9. The results of DNA quantification (Figure 5b) and CCK-8 assay (Figure 5c) further demonstrated that cell proliferation was higher in the ICA/GelMA and ICA/CS/GelMA groups than in the GelMA and CS/GelMA groups on days 1, 4, and 9, indicating that

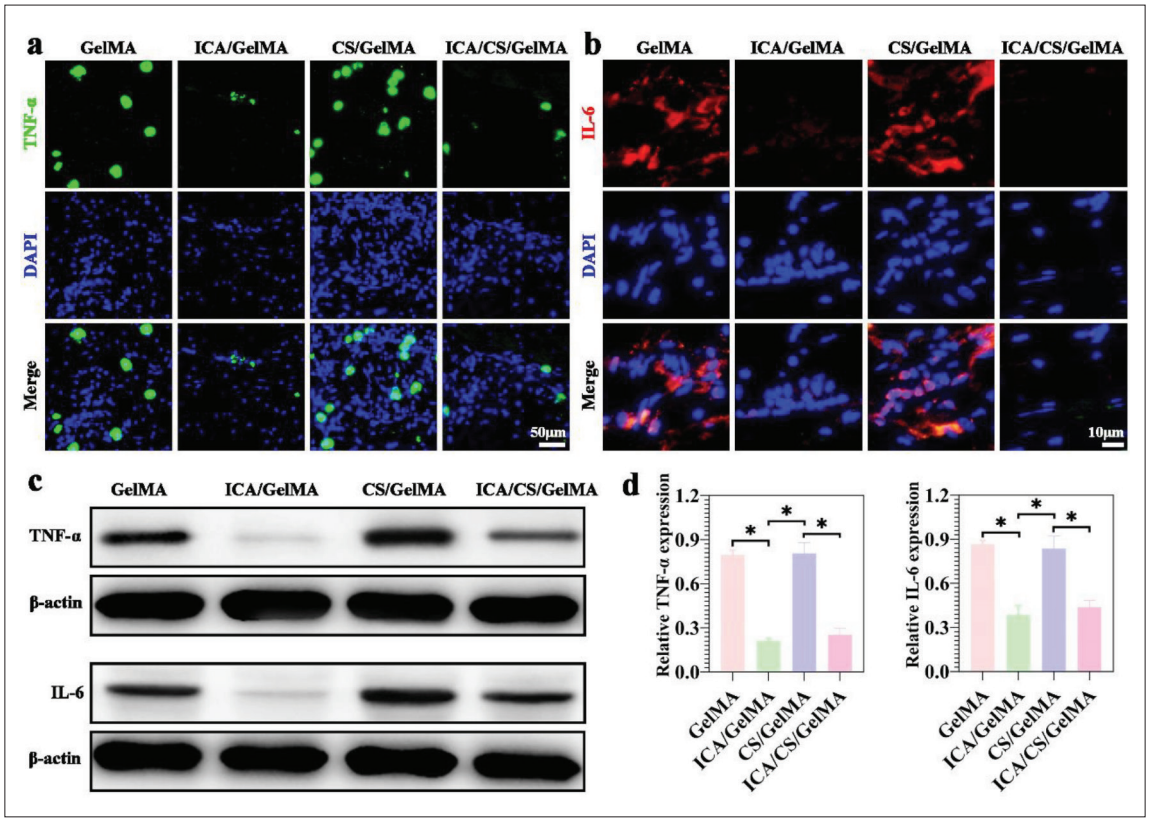

Figure 3. The anti-inflammatory ability of various hydrogels when incubated with pre-stimulated RAW264.7 macrophages for 24 h. Immunofluorescence staining was conducted to examine (a) TNF-α and (b) IL-6 expression levels in various hydrogel groups. (c) Relative protein expression levels of TNF-α and IL-6 were determined via western blotting analysis. (d) The relative gene expression levels of TNF-α and IL-6 were measured using qPCR examination. Statistical analysis was performed, and significance was indicated by asterisks (*$P < 0.05$).

the addition of ICA significantly promotes the proliferation of chondrocytes. Moreover, immunofluorescence staining and quantification for COL II content (Figure 5d–e) indicated that the ICA/GelMA and ICA/CS/GelMA groups showed more cartilage-specific ECM deposition than the GelMA and CS/GelMA groups after 3 weeks of *in vitro* culture.

These findings suggest that the addition of ICA enhances the chondrocyte viability, spreading, and proliferation, as well as the chondrogenic capacity of the ICA/GelMA and ICA/CS/GelMA groups, which may ultimately facilitate cartilage regeneration.

3.4. Anti-inflammatory evaluation of printed cell-laden hydrogels after submuscular implantation in autologous rabbits

To evaluate the anti-inflammatory function and cartilage regeneration capacity of the printed cell-laden hydrogels *in vivo*, C-shaped rings of various cell-laden hydrogel groups were implanted submuscularly onto a silicone tube in autologous rabbits for 3 and 6 weeks. Gross images showed that the ICA/GelMA and ICA/CS/GelMA groups exhibited interrupted cartilage-like tissue with smooth and shiny surfaces and ivory-white colors, whereas the GelMA and CS/GelMA groups appeared fibrosis-like with light-red colors (Figure 6a1–a8). Histological examination revealed more significant cartilage-specific ECM deposition in the ICA/GelMA and ICA/CS/GelMA groups compared to the GelMA and CS/GelMA groups at both 3 and 6 weeks, as evidenced by the presence of lacunar structures via H&E staining (Figure 6b1–b8), intensive Safranin-O staining (Figure 6c1–c8), and concentrated positive immunohistochemical COL II staining in the ICA/GelMA and ICA/CS/GelMA groups (Figure 6d1–d8). Additionally, the generated TETC in the ICA/GelMA and ICA/CS/GelMA groups had developed typical lacunae and a more homogeneous structure at 6 weeks. Quantitative data for GAG content and COL II content revealed higher levels in the ICA/GelMA and ICA/CS/GelMA groups than in the GelMA and CS/GelMA groups (Figure 6h–i), further validating that ICA/GelMA and ICA/CS/GelMA groups outperformed GelMA and CS/GelMA in cartilage regeneration *in vivo*.

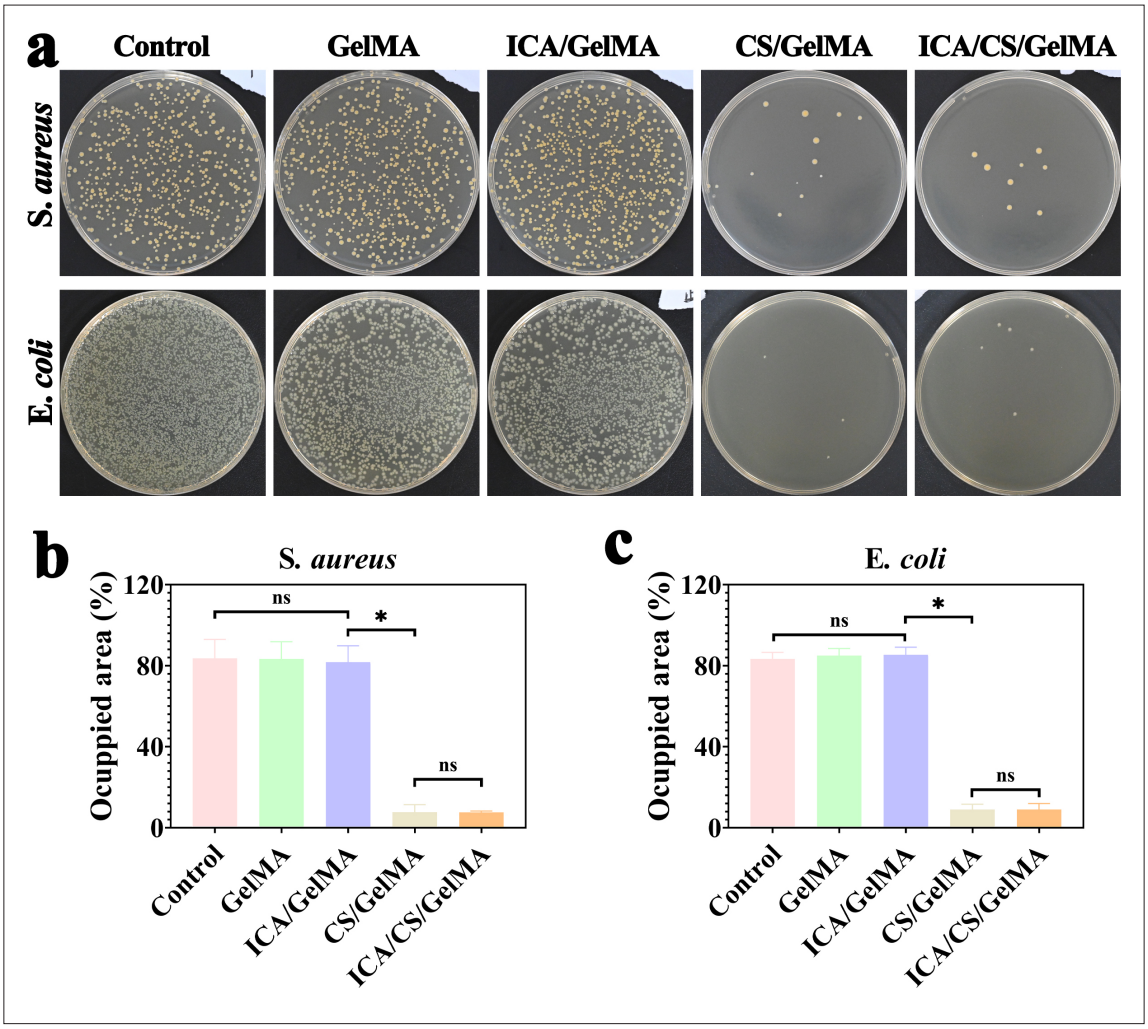

Figure 4. The anti-bacterial activity of GelMA, ICA/GelMA, CS/GelMA, and ICA/CS/GelMA hydrogels against S. aureus **and** E. coli**.** (a) Photographs of *S. aureus* and *E. coli* grown on agar plates after co-culturing with various hydrogels and control. The percentage of the occupied area of (b) *S. aureus* and (c) *E. coli* after co-culturing with various hydrogels and control was determined. Statistical analysis was performed, and significance was indicated by asterisks (*$P < 0.05$).

Immunofluorescence images of TNF-α and IL-6 (inflammatory-related cytokines) and TUNEL (apoptosis marker) were obtained to evaluate the inflammatory response. The GelMA and CS/GelMA groups exhibited intense positive staining for TNF-α, IL-6, and TUNEL compared to the ICA/GelMA and ICA/CS/GelMA groups at 3 and 6 weeks (Figure 6e1–e8, f1–f8, and g1–g8). The ICA/GelMA and ICA/CS/GelMA groups presented significantly lower TNF-α, IL-6, and TUNEL intensities than the GelMA and CS/GelMA groups (Figure 6j–l). These data supported the notion that ICA/GelMA and ICA/CS/GelMA hydrogels exhibit an advantage in reducing inflammatory reactions compared to GelMA and CS/GelMA hydrogels, which contribute to superior stability in maintaining tracheal cartilage.

3.5. Anti-bacterial assessment of TETC after orthotopically tracheal transplantation in autologous rabbit

Due to the insufficient mechanical properties of the GelMA and CS/GelMA groups for orthotopically tracheal transplantation, only the ICA/GelMA and ICA/CS/GelMA groups were used to evaluate the anti-bacterial effect in promoting tracheal defect restoration. The anti-bacterial ability of the generated TETC in the ICA/GelMA and ICA/CS/GelMA groups was evaluated by orthotopically transplanting the TETC into the tracheal defect of an autologous rabbit. The survival rate of experimental rabbits in the ICA/CS/GelMA group was significantly higher than in the ICA/GelMA group over the observed 8 weeks (Figure 7a). Gross images at 3 weeks post-transplantation revealed evident infection in the ICA/GelMA group, while

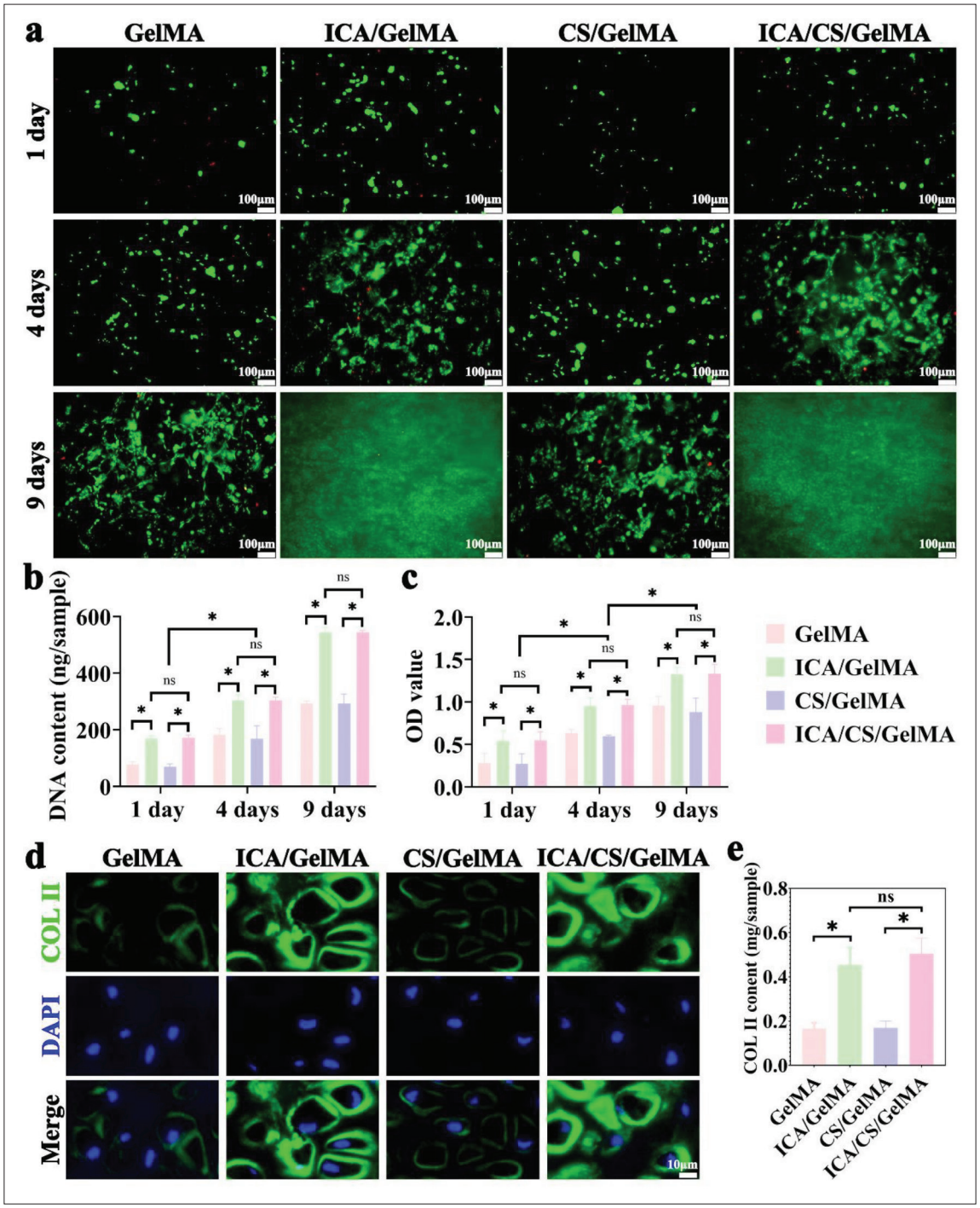

Figure 5. **The cytocompatibility and chondrogenic evaluations of GelMA, ICA/GelMA, CS/GelMA, and ICA/CS/GelMA hydrogels.** (a) Live/dead staining, (b) DNA quantification, and (c) CCK-8 assay were conducted on chondrocyte-laden hydrogels in various groups on days 1, 4, and 9. (d) Immunofluorescence staining and (e) quantification were performed to examine the COL II content in various chondrocyte-laden hydrogels after 3 weeks *in vitro* cultivation. Statistical analysis was performed, and significance was indicated by asterisks (*$P < 0.05$).

a relatively smooth lumen was seen in the ICA/CS/GelMA group (Figure 7b). Furthermore, immunofluorescence micrographs showed that more bacteria were present in the ICA/GelMA group than in the ICA/CS/GelMA group at 3 weeks (Figure 7c), which was confirmed by quantification of bacterial intensity (Figure 7d). Additionally, more cartilage ECM was preserved in the ICA/CS/GelMA group compared to the ICA/GelMA group at 3 weeks, as

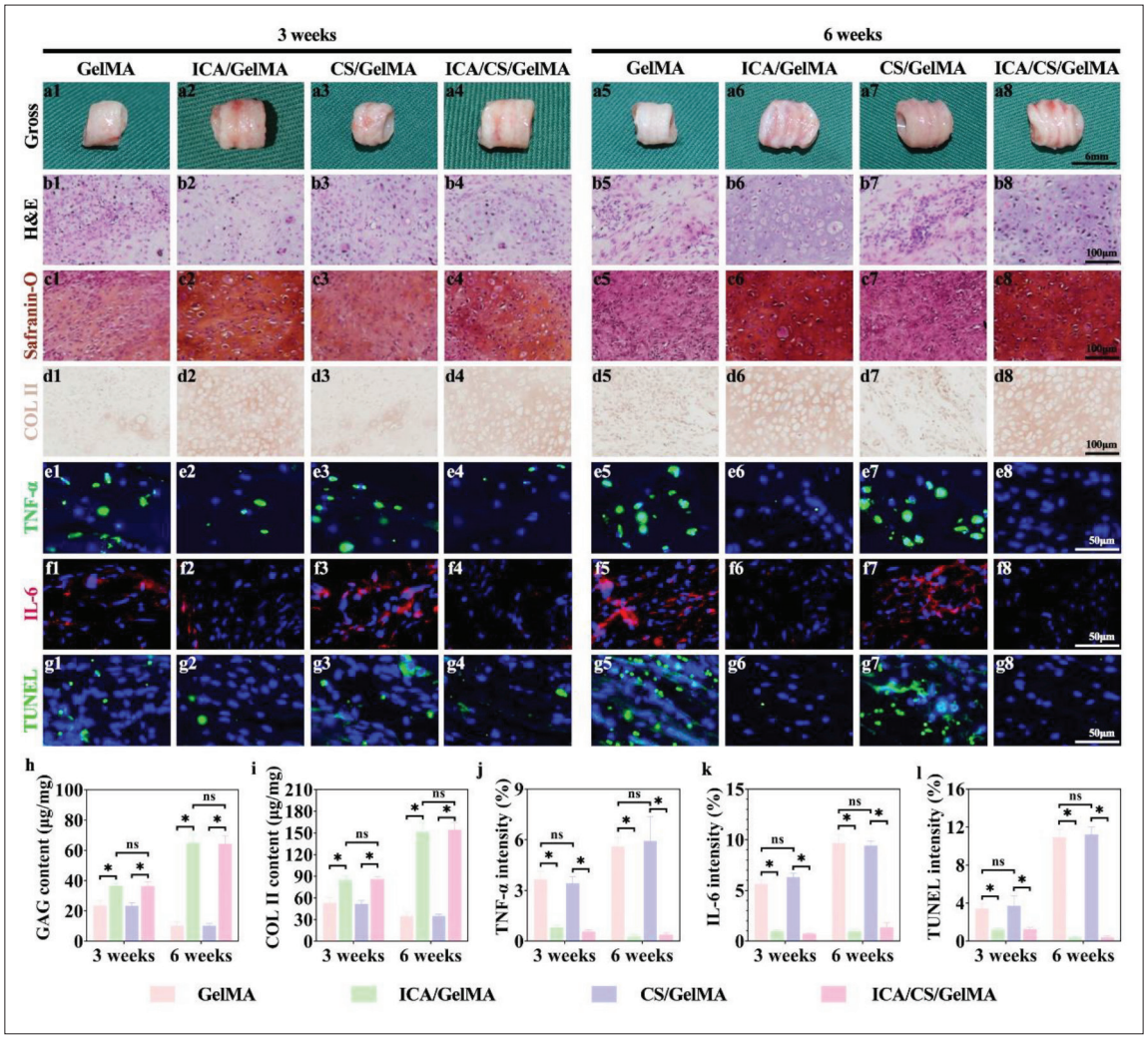

Figure 6. **The anti-inflammatory effect of various hydrogels for TETC formation at 3 and 6 weeks in a rabbit model.** (a1–a8) Gross observation, (b1–b8) H&E staining, (c1–c8) Safranin-O staining, (d1–d8) immunohistochemical COL II staining, and immunofluorescence staining of (e1–e8) TNF-α, (f1–f8) IL-6, and (g1–g8) TUNEL were conducted for TETC samples in GelMA, ICA/GelMA, CS/GelMA, and ICA/CS/GelMA groups. Quantitative measurements of (h) GAG and (i) COL II content, as well as relative (j) TNF-α, (k) IL-6, and (l) TUNEL intensity for TETC samples in GelMA, ICA/GelMA, CS/GelMA, and ICA/CS/GelMA groups were also presented. Statistical analysis was performed, and significance was indicated by asterisks (*$P < 0.05$).

evidenced by more intensive positive COL II expression in the ICA/CS/GelMA group than in the ICA/GelMA group (Figure 7c). Quantitative data revealed significantly higher COL II content and Young's modulus in the ICA/CS/GelMA group compared to the ICA/GelMA group (Figure 7e–f). These data support the notion that the ICA/CS/GelMA hydrogel exhibits an advantage in reducing bacterial infection compared to the ICA/GelMA hydrogel, which contributes to the enhanced therapeutic outcome in restoring tracheal cartilage defect.

4. Discussion

This study demonstrated that the synthesized ICA/CS/GelMA hydrogel possessed favorable rheological behavior, satisfactory gelation and swelling capabilities, and satisfactory cytocompatibility. Furthermore, the ICA/CS/GelMA hydrogel displayed potent *in vitro* anti-inflammatory capacity when co-cultured with LPS pre-stimulated RAW264.7 macrophages and impressive *in vitro* anti-bacterial effect when co-cultured with *S. aureus* and *E. coli*. Moreover, the chondrocyte-loaded ICA/CS/GelMA hydrogel was successfully 3D bioprinted into a precise C-shaped ring configuration. Additionally, the printed C-shaped rings in the ICA/CS/GelMA group demonstrated excellent *in vivo* anti-inflammatory function and developed a TETC tissue with C-shaped cartilage after being subcutaneously implanted into autologous rabbits for 6 weeks. Importantly, the generated TETC in the ICA/CS/GelMA group displayed satisfying *in vivo* anti-

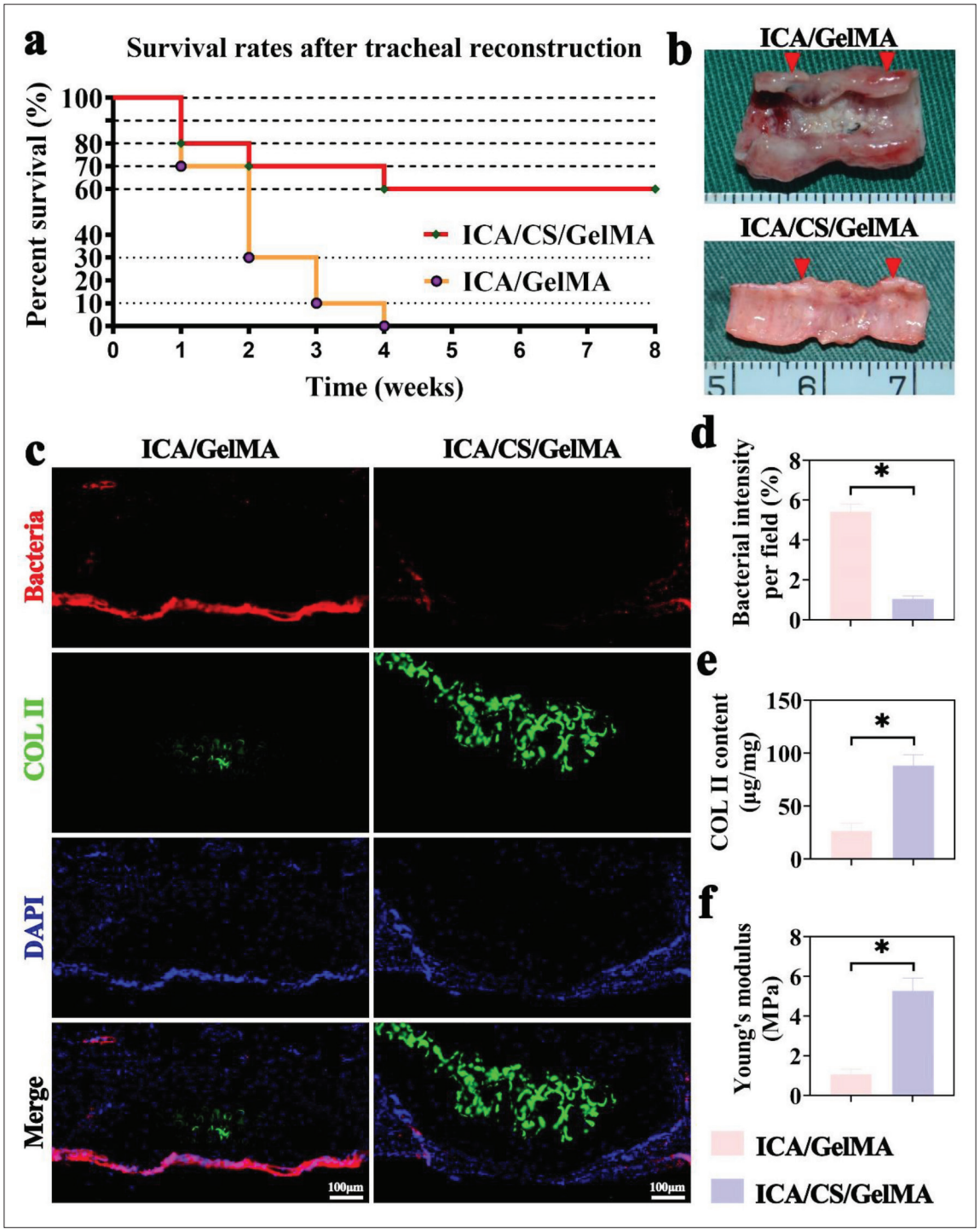

Figure 7. The anti-bacterial function of TETC in ICA/GelMA and ICA/CS/GelMA hydrogels after orthotopic tracheal transplantation in a rabbit model. (a) The survival rates of experimental rabbits in ICA/GelMA and ICA/CS/GelMA groups over 8 weeks post-transplantation are presented. (b) Gross observation of transplanted TETC in ICA/GelMA and ICA/CS/GelMA groups at 3 weeks is depicted, in which the red arrows indicate the interfaces between the implanted trachea and the native trachea. (c) Immunofluorescence images of bacteria and COL II for transplanted TETC in ICA/GelMA and ICA/CS/GelMA groups at 3 weeks are shown. (d–f) Quantitative measurements of (d) bacteria intensity, (e) COL II, and (f) Young's modulus for transplanted TETC in ICA/GelMA and ICA/CS/GelMA groups at 3 weeks are presented. Statistical analysis was conducted, and significance was indicated by asterisks (*$P < 0.05$).

bacterial activity and enhanced therapeutic effect after orthotopic tracheal transplantation in a rabbit model. In summary, these findings suggest that the ICA/CS/GelMA hydrogel is a suitable platform for 3D bioprinting with cells and exhibits both anti-inflammatory and anti-bacterial activities that can promote tracheal cartilage regeneration and restoration.

Recent research has emphasized the importance of achieving satisfactory tracheal cartilage regeneration for successful functional reconstruction of the trachea. However, several challenges, such as uneven chondrocyte distribution in the scaffold, difficult shape control, inevitable inflammatory reactions, and bacterial infections, have compromised the structure and functionality of TETC *in vivo*. In this study, we developed an ICA/CS/GelMA hydrogel that could be 3D bioprinted with chondrocytes to fabricate C-shaped rings with uniform chondrocyte distribution, thereby addressing the issues of chondrocyte distribution and shape control. The inclusion of ICA endowed the ICA/CS/GelMA hydrogel with anti-inflammatory properties, significantly enhancing TETC formation *in vivo*. Furthermore, the addition of CS imparted the ICA/CS/GelMA hydrogel with anti-bacterial properties, reducing bacterial infection and increasing the survival rate of experimental rabbits after orthotopic tracheal transplantation. Our findings suggest that this approach is a promising strategy for clinical translation in tracheal tissue engineering.

3D bioprinting is an innovative technology that offers high reproducibility and precise control over the fabrication of constructs in an automated manner. This technology has been employed to develop functional constructs for replacing damaged or injured tissues. In previous studies, two strategies were adopted to reconstruct tracheal cartilage: (i) seeding chondrocytes onto scaffolds and (2) using a molding method[1-6]. However, these strategies failed to overcome uneven cell distribution and chondrocyte wastage. To address these concerns, we have previously developed a new strategy for 3D bioprinting of a cartilage-vascularized fibrous tissue-integrated trachea. Although this approach enabled even distribution of chondrocytes in hydrogel and reduced chondrocyte wastage, the time-consuming 3D bioprinting process was detrimental to the survival of chondrocytes[18]. To overcome this challenge, we adopted a two-step strategy: (i) we separately 3D-bioprinted C-shaped chondrocyte-loaded hydrogel rings, which facilitated even distribution of chondrocytes in the hydrogel and required less total printing time compared to 3D printing a trachea-mimetic cellular construct, and (2) we reconstructed the tracheal cartilage using an *in vivo* bioreactor. Using an *in vivo* bioreactor allowed tissue fluid infiltration and vessel in-growth from the surrounding recipient tissue, which provided the necessary nutrients for the regeneration of the tracheal cartilage[31].

The inflammatory response of TETC is a significant concern *in vivo*, as it can be induced by various factors such as surgical trauma, biomaterials, and their degradation products, and it can considerably affect the stability of the cartilaginous phenotype[32,33]. Several studies have shown that this inflammatory reaction can lead to necrosis of engineered cartilage tissue, fibrosis, granulation hyperplasia, and, ultimately, failure of TETC after orthotopic tracheal transplantation[9,19,20]. Moreover, pro-inflammatory cytokines such as IL-6 and TNF-α can activate the NF-κB signaling pathway, causing local inflammation and apoptosis of tracheal tissues, particularly the cartilage[9,34]. In our current study, we observed high expression of inflammatory-related factors (TNF-α and IL-6), as well as apoptosis of chondrocytes (TUNEL), confirming that the inflammatory response was a crucial factor causing cartilage deterioration.

The airway mucosa plays a vital role in preventing infections and performing key physiological functions, such as the clearance of secretions via the mucociliary escalator. Minor injuries involving limited surface areas can be self-repaired through epithelial migration from the wound edge. However, the epithelialization of TETC through self-migration of adjacent epithelium is time-consuming and unreliable[35]. Studies have shown that inflammation caused by bacterial infections can severely compromise TETC due to a lack of airway mucosa[1-6]. This can lead to airway obstruction and excess mucus, supporting the colonization of potential pathogens such as *Pseudomonas aeruginosa*, and increasing mortality in experimental animals. However, few studies have investigated the impact of anti-bacterial effects on TETC. It is well-established that the upper respiratory tract of healthy individuals is continuously colonized by microbes[36]. Researchers have suggested that defects in mucociliary clearance, as well as airway macrophage and neutrophil dysfunction, may contribute to inflammation progression and exacerbation[37]. In this study, we discovered that anti-bacterial effects may contribute to maintaining the cartilaginous phenotype and promoting tracheal cartilage formation. It is worth noting that despite the demonstrated superior anti-bacterial efficacy of the ICA/CS/GelMA group at the third week, there was a significant mortality rate of 30% observed among rabbits in this group during the 1st to 3rd weeks following transplantation. This observation led us to speculate that the released CS from the ICA/CS/GelMA group might not adequately fulfill the essential functions of the tracheal epithelium, such as mucus-based trapping of toxic particles

and their subsequent clearance from the respiratory tract via cilia movement[38]; therefore, further investigations are warranted to simulate the functionality of healthy airway epithelium in future studies.

GelMA hydrogel has gained significant attention due to its tunable mechanical properties, excellent biocompatibility, ability to mimic the microenvironment of the native ECM, and its potential as a carrier for cells and drug molecules[16,29]. In our current study, we mixed 10 μM ICA and 2% w/v CS into 10% w/v GelMA hydrogel to obtain an effective anti-inflammatory and anti-bacterial property and then 3D-bioprinted the C-shaped chondrocyte-laden hydrogel rings[16,39,40]. The results, including high expression of inflammatory-related factors (TNF-α and IL-6), chondrocyte apoptosis (TUNEL), anti-bacterial activity, and gross and histological view (fibrosis and granulation hyperplasia), consistently verified that anti-inflammatory and anti-bacterial effects could contribute to maintaining the cartilaginous phenotype and promoting tracheal cartilage formation. Several contributing factors may explain these results: (i) The 3D-bioprinted C-shaped hydrogel ring exhibited uniform distribution of chondrocytes and demanded less total printing time, which significantly enhanced cell viability and functionality of the trachea-mimetic cellular construct, including its differentiation capacity into tracheal cartilage[17]; (ii) our previous study found that C-shaped cartilage has better compliance to increase airflow velocity and mucous transport, which evidently contributed to maintenance of lumen patency[6,41]; (iii) ICA has been proven to exert favorable anti-inflammatory and chondroprotective effects by modulating autophagy and apoptosis[25,26]; (iv) ICA also showed chondrogenic effects, including promoting chondrocyte proliferation and ECM synthesis[27]; (v) CS, which possesses excellent anti-bacterial abilities and has been approved by the FDA for pharmaceutical applications, effectively protected TETC from infection; (vi) the synergistic effect of ICA and CS was conducive to suppressing inflammation caused by infection, indirectly enhancing the anti-inflammatory function of ICA; and (vii) the released ICA and CS from the ICA/CS/GelMA hydrogel can sustainably promote chondrocyte proliferation and ECM synthesis, anti-inflammatory and anti-bacterial effects with the degradation of GelMA.

Although our current study successfully demonstrated the potential of 3D-bioprinting technology to fabricate C-shaped chondrocyte-laden ICA/CS/GelMA hydrogel rings for enhancing tracheal cartilage regeneration and restoration, several limitations still need to be addressed in future research. Firstly, although we found that reducing printing time significantly enhanced cell viability and functionality of the trachea-mimetic cellular construct, including its differentiation capacity into tracheal cartilage, more advanced 3D bioprinting strategies need to be explored to create a more complete trachea-mimetic cellular construct with improved cell viability and functionality. Secondly, although the anti-bacterial ability of the ICA/CS/GelMA hydrogel was initially verified, researchers still need to make further efforts to elucidate the specific mechanism of anti-bacterial effects on reconstructing segmental tracheal defects.

5. Conclusion

In conclusion, our current study developed a novel cell-laden hydrogel with anti-inflammatory and anti-bacterial activities for tracheal cartilage regeneration and restoration using a 3D-bioprinting strategy. We confirmed that the ICA/CS/GelMA hydrogel exhibited rheological behavior, photo-triggered gelation, suitable printability, favorable biocompatibility, and simulated microenvironments for chondrogenesis. Moreover, the ICA/CS/GelMA hydrogel exerted favorable anti-inflammatory and anti-bacterial effects both *in vitro* and *in vivo*, resulting in a significant enhancement in tracheal cartilage regeneration and restoration, as well as a significant increase in the survival rate of experimental rabbits after orthotopic transplantation. Although several limitations still need to be addressed in future research, this study suggests that 3D-bioprinted cell-laden ICA/CS/GelMA hydrogel with anti-inflammatory and anti-bacterial activities is a promising candidate for enhancing tracheal cartilage regeneration and restoration.

Acknowledgments

None.

Funding

The research was supported by the National Natural Science Foundation of China (82102348) and the Natural Science Foundation of Shanghai (22YF1437400).

Conflict of Interest

The authors declare no conflict of interest.

Author contributions

Conceptualization: Pengli Wang
Data curation: Pengli Wang
Formal analysis: Tao Wang
Funding acquisitions: Yong Xu, Xue Zhang
Investigation: Pengli Wang
Methodology: Tao Wang
Project administration: Nan Song
Resources: Nan Song

Supervision: Xue Zhang
Visualization: Xue Zhang
Writing – original draft: *Pengli Wang*
Writing – review & editing: Pengli Wang

Ethics approval and consent to participate

Ethical approval was obtained from the Experimental Animal Ethics Committee of Shanghai Pulmonary Hospital (K21-355Y).

Consent for publication

Not applicable.

Availability of data

The data that support the findings of this study are available from the corresponding author upon reasonable request.

References

1. Xu Y, Li D, Yin ZQ, *et al.*, 2017, Tissue-engineered trachea regeneration using decellularized trachea matrix treated with laser micropore technique. *Acta Biomater*, 58: 113–121.

   http://doi.org/10.1016/j.actbio.2017.05.010

2. Xu Y, Duan H, Li YQ, *et al.*, 2020, Nanofibrillar decellularized Wharton's jelly matrix for segmental tracheal repair. *Adv Funct Mater*, 30(14): 1910067.

   http://doi.org/10.1002/adfm.201910067

3. Xu Y, Dai J, Zhu XS, *et al.*, 2022, Biomimetic trachea engineering via a modular ring strategy based on bone-marrow stem cells and atelocollagen for use in extensive tracheal reconstruction. *Adv Mater*, 34(6): 2106755.

   http://doi.org/10.1002/adma.202106755

4. Gao E, Li G, Cao RF, *et al.*, 2022, Bionic tracheal tissue regeneration using a ring-shaped scaffold comprised of decellularized cartilaginous matrix and silk fibroin. *Compos Part B-Eng*, 229: 109470.

   http://doi.org/10.1016/j.compositesb.2021.109470

5. Xu Y, Guo Y, Li Y, *et al.*, 2020, Biomimetic trachea regeneration using a modular ring strategy based on poly(sebacoyl diglyceride)/polycaprolactone for segmental trachea defect repair. *Adv Funct Mater*, 30(42): 2004276.

   http://doi.org/10.1002/adfm.202004276

6. Gao ER, Wang Y, Wang PL, *et al.*, 2023, C-shaped cartilage development using Wharton's jelly-derived hydrogels to assemble a highly biomimetic neotrachea for use in circumferential tracheal reconstruction. *Adv Funct Mater*, 33(14) 2212830.

   http://doi.org/10.1002/adfm.202212830

7. Hong H, Seo YB, Kim DY, *et al.*, 2020, Digital light processing 3D printed silk fibroin hydrogel for cartilage tissue engineering. *Biomaterials*, 232: 119679.

   http://doi.org/10.1016/j.biomaterials.2019.119679

8. Kandi R, Sachdeva K, Choudhury SD, *et al.*, 2023, A facile 3D bio-fabrication of customized tubular scaffolds using solvent-based extrusion printing for tissue-engineered tracheal grafts. *J Biomed Mater Res A*, 111(2): 278–293.

   http://doi.org/10.1002/jbm.a.37458

9. Yang ML, Sun WY, Wang L, *et al.*, 2022, Curcumin loaded polycaprolactone scaffold capable of anti-inflammation to enhance tracheal cartilage regeneration. *Mater Design*, 224: 111299.

   http://doi.org/10.1016/j.matdes.2022.111299

10. Bush A, Floto RA, 2019, Pathophysiology, causes and genetics of paediatric and adult bronchiectasis. *Respirology*, 24(11): 1053–1062.

    http://doi.org/10.1111/resp.13509

11. Kolwijck E, van de Veerdonk FL, 2014, The potential impact of the pulmonary microbiome on immunopathogenesis of Aspergillus-related lung disease. *Eur J Immunol*, 44(11): 3156–3165.

    http://doi.org/10.1002/eji.201344404

12. Dhasmana A, Singh A, Rawal S, 2020, Biomedical grafts for tracheal tissue repairing and regeneration "Tracheal tissue engineering: an overview". *J Tissue Eng Regen Med*, 14(5): 653–672.

    http://doi.org/10.1002/term.3019

13. Reynolds PM, Holzmann Rasmussen C, Hansson M, *et al.*, 2018, Controlling fluid flow to improve cell seeding uniformity. *PLoS One*, 13(11): e0207211.

    http://doi.org/10.1371/journal.pone.0207211

14. Xu Y, Wang Z, Hua Y, *et al.*, 2021, Photocrosslinked natural hydrogel composed of hyaluronic acid and gelatin enhances cartilage regeneration of decellularized trachea matrix. *Mater Sci Eng C Mater Biol Appl*, 120: 111628.

    http://doi.org/10.1016/j.msec.2020.111628

15. Xu Y, Li Y, Liu Y, *et al.*, 2019, Surface modification of decellularized trachea matrix with collagen and laser micropore technique to promote cartilage regeneration. *Am J Transl Res*, 11(9): 5390–5403.

16. Lazaridou M, Bikiaris DN, Lamprou DA, 2022, 3D bioprinted chitosan-based hydrogel scaffolds in tissue engineering and localised drug delivery. *Pharmaceutics*, 14(9): 1978.

    http://doi.org/10.3390/pharmaceutics14091978

17. Park JH, Ahn M, Park SH, *et al.*, 2021, 3D bioprinting of a trachea-mimetic cellular construct of a clinically relevant size. *Biomaterials*, 279: 121246.

    http://doi.org/10.1016/j.biomaterials.2021.121246

18. Huo Y, Xu Y, Wu X, *et al.*, 2022, Functional trachea reconstruction using 3D-bioprinted native-like tissue architecture based on designable tissue-specific bioinks. *Adv Sci (Weinh)*, 9(29): e2202181.

    http://doi.org/10.1002/advs.202202181

19. Liu Y, Li D, Yin Z, *et al.*, 2016, Prolonged in vitro precultivation alleviates post-implantation inflammation and promotes stable subcutaneous cartilage formation in a goat model. *Biomed Mater*, 12(1): 015006.

    http://doi.org/10.1088/1748-605X/12/1/015006

20. Luo X, Zhou G, Liu W, *et al.*, 2009, In vitro precultivation alleviates post-implantation inflammation and enhances development of tissue-engineered tubular cartilage. *Biomed Mater*, 4(2): 025006.

    http://doi.org/10.1088/1748-6041/4/2/025006

21. Gao E, Wang P, Chen F, *et al.*, 2022, Skin-derived epithelial lining facilitates orthotopic tracheal transplantation by protecting the tracheal cartilage and inhibiting granulation hyperplasia. *Biomater Adv*, 139: 213037.

    http://doi.org/10.1016/j.bioadv.2022.213037

22. Jungebluth P, Moll G, Baiguera S, *et al.*, 2012, Tissue-engineered airway: a regenerative solution. *Clin Pharmacol Ther*, 91(1): 81–93.

    http://doi.org/10.1038/clpt.2011.270

23. Dikina AD, Strobel HA, Lai BP, *et al.*, 2015, Engineered cartilaginous tubes for tracheal tissue replacement via self-assembly and fusion of human mesenchymal stem cell constructs. *Biomaterials*, 52: 452–462.

    http://doi.org/10.1016/j.biomaterials.2015.01.073

24. Lei D, Luo B, Guo YF, *et al.*, 2019, 4-Axis printing microfibrous tubular scaffold and tracheal cartilage application. *Sci China Mater*, 62(12): 1910–1920.

    http://doi.org/10.1007/s40843-019-9498-5

25. Cao Y, 2021, Icariin alleviates MSU-induced rat GA models through NF-kappaB/NALP3 pathway. *Cell Biochem Funct*, 39(3): 357–366.

    http://doi.org/10.1002/cbf.3598

26. Mi B, Wang J, Liu Y, *et al.*, 2018, Icariin activates autophagy via down-regulation of the NF-kappaB signaling-mediated apoptosis in chondrocytes. *Front Pharmacol*, 9: 605.

    http://doi.org/10.3389/fphar.2018.00605

27. Oprita EI, Iosageanu A, Craciunescu O, 2022, Progress in composite hydrogels and scaffolds enriched with icariin for osteochondral defect healing. *Gels*, 8(10): 648.

    http://doi.org/10.3390/gels8100648

28. Qi W, Dong N, Wu L, *et al.*, 2023, Promoting oral mucosal wound healing using a DCS-RuB(2)A(2) hydrogel based on a photoreactive antibacterial and sustained release of BMSCs. *Bioact Mater*, 23: 53–68.

    http://doi.org/10.1016/j.bioactmat.2022.10.027

29. Xiang L, Cui W, 2021, Biomedical application of photo-crosslinked gelatin hydrogels. *J Leather Sci Eng*, 3(1): 3.

    http://doi.org/10.1186/s42825-020-00043-y

30. Zhang M, Zhu JY, Qin X, *et al.*, 2019, Cardioprotection of tetrahedral DNA nanostructures in myocardial ischemia-reperfusion injury. *Acs Appl Mater Inter*, 11(34): 30631–30639.

    http://doi.org/10.1021/acsami.9b10645

31. Xu Y, Guo Z, Liu R, *et al.*, 2020, Bioengineered carina reconstruction using in-vivo bioreactor technique in human: Proof of concept study. *Transl Lung Cancer Res*, 9(3): 705–712.

    http://doi.org/10.21037/tlcr-20-534

32. Murphy MP, Koepke LS, Lopez MT, *et al.*, 2020, Articular cartilage regeneration by activated skeletal stem cells. *Nat Med*, 26(10): 1583.

    http://doi.org/10.1038/s41591-020-1013-2

33. Wu CL, Harasymowicz NS, Klimak MA, *et al.*, 2020, The role of macrophages in osteoarthritis and cartilage repair. *Osteoarthr Cartilage*, 28(5): 544–554.

    http://doi.org/10.1016/j.joca.2019.12.007

34. Koh RH, Jin Y, Kim J, *et al.*, 2020, Inflammation-modulating hydrogels for osteoarthritis cartilage tissue engineering. *Cells*, 9(2): 419.

    http://doi.org/10.3390/cells9020419

35. Hamilton N, Bullock AJ, Macneil S, *et al.*, 2014, Tissue engineering airway mucosa: A systematic review. *Laryngoscope*, 124(4): 961–968.

    http://doi.org/10.1002/lary.24469

36. Wypych TP, Wickramasinghe LC, Marsland BJ, 2019, The influence of the microbiome on respiratory health. *Nat Immunol*, 20(10): 1279–1290.

    http://doi.org/10.1038/s41590-019-0451-9

37. Mindt BC, DiGiandomenico A, 2022, Microbiome modulation as a novel strategy to treat and prevent respiratory infections. *Antibiotics (Basel)*, 11(4): 474.

    http://doi.org/10.3390/antibiotics11040474

38. Maurizi E, Adamo D, Magrelli FM, *et al.*, 2021, Regenerative medicine of epithelia: Lessons from the past and future goals. *Front Bioeng Biotechnol*, 9: 652214.

    http://doi.org/10.3389/fbioe.2021.652214

39. Rahimnejad M, Adoungotchodo A, Demarquette NR, *et al.*, 2022, FRESH bioprinting of biodegradable chitosan thermosensitive hydrogels. *Bioprinting*, 27: e00209.

40. Zhu Y, Ye L, Cai X, *et al.*, 2022, Icariin-loaded hydrogel regulates bone marrow mesenchymal stem cell chondrogenic differentiation and promotes cartilage repair in osteoarthritis. *Front Bioeng Biotechnol*, 10: 755260.

http://doi.org/10.3389/fbioe.2022.755260.

41. Luo X, Liu Y, Zhang Z, *et al.*, 2013, Long-term functional reconstruction of segmental tracheal defect by pedicled tissue-engineered trachea in rabbits. *Biomaterials*, 34(13): 3336–3344.

http://doi.org/10.1016/j.biomaterials.2013.01.060